Chemico-Biological Interactions 203 (2013) 412–422

Contents lists available at SciVerse ScienceDirect

Chemico-Biological Interactions

journal homepage: www.elsevier.com/locate/chembioint

# Evidence of securin-mediated resistance to gefitinib-induced apoptosis in human cancer cells

Sheng-Yi Yu [a,1], Huei-Fang Liu [b,1], Su-Pei Wang [b], Chia-Ching Chang [b], Chuan-Mei Tsai [b], Jui-I Chao [a,b,*]

[a] Institute of Molecular Medicine and Bioengineering, National Chiao Tung University, Hsinchu 300, Taiwan
[b] Department of Biological Science and Technology, National Chiao Tung University, Hsinchu 300, Taiwan

ARTICLE INFO

*Article history:*
Received 5 December 2012
Received in revised form 14 February 2013
Accepted 9 March 2013
Available online 22 March 2013

*Keywords:*
Gefitinib
Securin
Apoptosis
EGFR
Cancer cells

ABSTRACT

Gefitinib, a tyrosine kinase inhibitor of the epidermal growth factor receptor (EGFR), has been used to treat numerous cancers; however, evidence has shown that cancer cells can become resistant to gefitinib during therapy. Here, we report a human proto-oncogene, securin, which displays resistance to death in cancer cells. Gefitinib treatment decreases securin levels at the protein level by inducing protein instability but did not affect on the securin gene expression. Treatment with gefitinib induced cytotoxicity in various human cancer cell types, including RKO (colon cancer), A549 (lung cancer), BFTC905 (bladder cancer), MCF7 (breast cancer) and A375 (skin cancer). BFTC905 and A549 cells expressed relatively high levels of the phosphorylated and total EGFR proteins; however, A375, MCF7 and RKO cells did not markedly express these proteins. Moreover, following treatment with gefitinib, the securin-wild type cancer cells were more resistant to apoptotic induction than the securin-null cancer cells. Surprisingly, both the securin-wild type and securin-null cancer cells expressed the EGFR protein at similar levels. Treatment with gefitinib induced mitochondrial dysfunction, cytochrome c release, caspase-3 activation and poly (ADP-ribose) polymerase protein cleavage, indicating that apoptosis occurred in these cancer cells. The transfection of a GPF–securin expression vector increased both the proliferation rates and resistance to gefitinib-induced death in these cancer cells. Taken together, these findings demonstrate that the presence of securin promotes resistance to gefitinib-induced apoptosis via an EGFR-independent pathway in human cancer cells.



## 1. Introduction

Epidermal growth factor receptor (EGFR) is composed of an extracellular ligand-binding domain, a transmembrane domain and an intracellular tyrosine kinase domain [1,2]. Abnormal EGFR expression promotes tumor progression [3,4]. The inhibition of EGFR has been used in cancer targeting therapeutics [5–7]. Gefitinib (Iressa, ZD-1839), a small molecule tyrosine kinase inhibitor of EGFR, has been used to treat various human cancers, such as lung and colon cancers [6,7]. Gefitinib can inhibit cancer cell proliferation [4,8] and induce apoptosis [8–10]. However, several reports show that cancer cells can become resistant to gefitinib and other EGFR inhibitors during cancer therapy [11–14]. It has been shown that cancers can be induced by activating mutations in EGFR and are responsive to tyrosine kinase inhibitors. Unfortunately, the efficacy of these drugs is often limited by a second mutation T790M of EGFR in lung cancer cells [15]. The T790M mutation in EGFR causes drug resistance by increasing the binding affinity for ATP [15]. Elucidating the mechanisms of resistance to such drugs in cancer cells will be beneficial for cancer patient treatment using EGFR inhibitors.

Securin is also referred to as the pituitary-tumor transforming gene (PTTG) [16–18]. Under normal conditions, securin is a mitotic regulator that prevents abnormal chromosome segregation [19,20]. However, securin has been shown to be highly expressed in a variety of human cancers [21], including pituitary [22], colon [23], breast [24], lung [25], and ovarian cancers [26]. The blockage of securin can reduce cancer cell survival [27–29]. The levels of securin have been correlated with tumorigenesis and cancer metastasis [21,22,30–32]. In addition, the presence of securin correlates with poor patient prognosis in response to cancer therapy [33,34].

*Abbreviations:* EGFR, epidermal growth factor receptor; EGF, epidermal growth factor; PTTG, pituitary-tumor transforming gene; DMSO, dimethyl sulfoxide; PI, propidium iodide; MTT, 3-(4,5-dimethyl-thiazol-2-yl) 2,5-diphenyl tetrazolium bromide; DiOC6, 3,3′-dihexiloxadicarbocyanine; PARP, poly(ADP-ribose) polymerase; FITC, fluorescein isothiocyanate; FBS, fetal bovine serum; PBS, phosphate-buffered saline; RT-PCR, reverse transcription-polymerase chain reaction; GFP, green fluorescence protein.

* Corresponding author at: Department of Biological Science and Technology, National Chiao Tung University, 75, Bo-Ai Street, Hsinchu 30068, Taiwan. Fax: +886 3 5556219.
*E-mail address:* jichao@faculty.nctu.edu.tw (J.-I Chao).
[1] Both the authors equally contributed to this study.

0009-2797/$ - see front matter © 2013 Elsevier Ireland Ltd. All rights reserved.
http://dx.doi.org/10.1016/j.cbi.2013.03.011

EGFR has been shown to be associated with securin gene expression, which enhances the proliferation of pituitary folliculostellate cells [35]. Gefitinib could block the EGF-induced securin expression and cellular proliferation [35]. Another EGFR inhibitor, AG1478, has also been shown to inhibit securin induction [36]. However, the reason for the presence of securin and the mechanism for its resistance to EGFR inhibitor-induced cancer cell death need to be explained.

In the present study, we have found that gefitinib reduces securin levels by inducing protein instability and does not affect its gene expression levels in cancer cells. The presence of securin in cancer cells could reduce gefitinib-induced cell death. We provide evidence of securin-mediated resistance to gefitinib-induced apoptosis in human cancer cells. Furthermore, securin promotes resistance to gefitinib-induced apoptosis in an EGFR-independent pathway.

## 2. Materials and methods

### 2.1. Reagents and antibodies

Gefitinib was purchased from proteinkinase.de (Biaffin GmbH and Co KG, Kassel, Germany) and was dissolved in dimethyl sulfoxide (DMSO). Propidium iodide (PI), 3-(4,5-dimethyl-thiazol-2-yl)-2,5-diphenyl tetrazolium bromide (MTT), the Cy3-labeled mouse anti-β-tubulin (c-4585), and Hoechst 33258 were purchased from Sigma Chemical Co. (St. Louis, MO, USA). 3,3′-Dihexyloxadicarbocyanine (DiOC6) was purchased from Calbiochem (San Diego, CA, USA). BODIPY FL phallacidin (B-607) was purchased from Invitrogen (Carlsbad, CA, USA). Anti-phospho-EGFR (05-1128) and anti-EGFR (05-104) antibodies were purchased from Millipore (Temecula, CA, USA). Anti-caspase-3 antibody (3004-100) was purchased from BioVision Research Products (Mountain View, CA, USA). Anti-poly(ADP-ribose) polymerase (PARP) (#9542), cytochrome c, and COX IV antibodies were purchased from Cell Signaling Technology, Inc. (Beverly, MA, USA). Anti-securin (ab-3305) antibody was purchased from Abcam (Cambridgeshire, UK). FITC (fluorescein isothiocyanate)-labeled goat anti-mouse IgG (sc-2010) and anti-ERK-2 (C-14) antibodies were purchased from Santa Cruz Biotechnology, Inc. (Santa Cruz, CA, USA). Anti-actin (MAB1501) antibody was purchased from Chemicon International, Inc. (Temecula, CA, USA).

### 2.2. Cell culture

RKO is a colorectal carcinoma cell line. The A549 cell line was derived from lung carcinoma. BFTC905 cells were derived from bladder carcinoma. The MCF7 cell line was derived from breast adenocarcinoma. A375 cells were derived from a malignant melanoma skin carcinoma. The A431 cell line was derived from an epidermoid carcinoma that highly expressed the EGFR proteins. RKO, A375 and A431 cells were maintained in DMEM medium (Gibco, Life Technologies, Grand Island, NY). A549, BFTC905 and MCF7 cells were cultured in RPMI-1640 medium (Gibco, Life Technologies). The securin-wild type and the securin-null HCT116 colorectal carcinoma cells were cultured in McCoy's 5A medium (Sigma Chemical). The complete medium was supplemented with 10% fetal bovine serum (FBS), with 100 units/ml of penicillin, and 100 μg/ml of streptomycin and sodium bicarbonate. These cells were maintained at 37 °C and 5% $CO_2$ in a humidified incubator (310/Thermo, Forma Scientific, Inc., Marietta, OH).

### 2.3. Cytotoxicity assay

The cells were plated in 96-well plates at a density of $1 \times 10^4$ cells/well for 16–20 h. Following a 24 h treatment with gefitinib, the cells were washed with phosphate-buffered saline (PBS), replated with fresh medium and cultured for 2 days. Thereafter, the medium was replaced, and the cells were incubated with 0.5 mg/ml of MTT in complete medium for 4 h. The surviving cells converted MTT to formazan, which generates a blue-purple color when dissolved in dimethyl sulfoxide. The intensity of formazan was measured at 565 nm using a plate reader (VERSAmax, Molecular Devices). The relative cell viability was calculated by dividing the absorbance of treated cells by that of the control in each experiment.

### 2.4. Cell cycle analysis

The cell cycle progression after treatment with gefitinib was measured by flow cytometry. The cells were plated at a density of $1 \times 10^6$ cells per 60-mm Petri dish in complete medium overnight. Then, the cells were treated with 0–60 μM gefitinib for 24 h. At the end of the treatment, the cells were collected and fixed with ice-cold 70% ethanol overnight at −20 °C. After centrifugation, the cell pellets were treated with 4 μg/ml PI solution containing 1% Triton X-100 and 100 μg/ml RNase at 37 °C for 30 min (in the dark). After re-centrifugation, the cells were resuspended in 1 ml of ice-cold PBS. To avoid cell aggregation, the cell solutions were filtered through nylon membranes. Subsequently, the samples were analyzed on a flow cytometer (FACSCalibur, BD Biosciences, San Jose, CA). A minimum of ten thousand cells were analyzed for DNA content, and the percentage of cell cycle phases was quantified using ModFit LT software (Ver. 2.0, BD Biosciences).

### 2.5. Annexin V and PI assays

An annexin V-PI staining kit (BioVision, Mountain View, CA) was used to examine the cells. The cells were incubated with FITC-conjugated-annexin V and PI according to the manufacturer's instructions. The cells were cultured in 60-mm Petri dishes at a density of $1 \times 10^6$ cells for overnight. After treatment with or without gefitinib for 24 h, the cells were washed with PBS. The cells were trypsinized and collected by centrifugation at 1500 rpm for 5 min. Thereafter, the cells were incubated with 500 μL of the annexin V-PI labeling solution. Finally, the samples were analyzed by flow cytometry using CellQuest software (FACSCalibur, BD Biosciences). The cells showed populations of annexin V(+)/PI(−) and annexin V(+)/PI(+), which indicated the cells undergoing early and late apoptosis, respectively.

### 2.6. Time-lapse observation of cell death

The cells were plated at a density of $2 \times 10^5$ cells/35-mm Petri dish for 24 h. Thereafter, the cells were exposed to 60 μM gefitinib or the control for 24 h. Any alteration in cell morphology was recorded by an imaging system composed of an inverted microscope (OLYMPUS, IX71, Japan) within a cell culture incubator. The cell morphology of apoptosis was confirmed by observation of the round-up morphology, the cell membrane blebbing and the formation of apoptotic bodies under phase contrast microscope.

### 2.7. Mitochondrial membrane potential

Mitochondrial function was evaluated by staining the cells with the mitochondrial sensitive probe DiOC6. The lipophilic cation DiOC6 accumulates in the mitochondrial matrix due to the electrochemical gradient. The cells were cultured in 60-mm Petri dishes at a density of $1 \times 10^6$ cells overnight. After treatment with or without gefitinib, the cells were washed with ice-cold PBS. The cells were trypsinized and collected by centrifugation. Then, the cell pellets were incubated with 50 nM DiOC6 in complete medium at 37 °C for 30 min (in the dark). Finally, the cell pellets were col-

lected by centrifugation and resuspended in 1 ml of ice-cold PBS and analyzed by a flow cytometer (FACSCalibur, BD Biosciences).

### 2.8. Separation of mitochondrial and cytosolic fractions

To examine the effect of gefitinib on cytochrome c release from mitochondria, the mitochondrial and cytosolic fractions of cells were separated by Mitochondria/Cytosol Fractionation kit (BioVision Inc., Mountain View, CA). A375 cells were cultured in 100-mm Petri dish at a density of $1 \times 10^7$ cells for 16–20 h. After treatment with or without gefinitib for 24 h, the cells were washed with PBS. Thereafter, the cells were collected. The cell pellet was resuspended in 10 ml ice-cold PBS and collected by centrifugation at 600*g* for 5 min. The cells were lysed in 500 μl extraction buffer containing dithiothreitol and protease inhibitor cocktail on ice for 10 min and vortexed cells for 30 min at 4 °C. The homogenate was centrifuged at 3000 rpm for 10 min at 4 °C. The supernatant was transferred into a new tube and centrifuged at 13,000 rpm for 30 min at 4 °C. The supernatant was carefully removed and collected as the cytosolic fraction and the remaining mitochondrial pellet was resuspended in the mitochondrial extraction buffer. The protein levels of cytochrome c in the mitochondrial and cytosolic fractions were subjected to Western blot analysis.

### 2.9. Western blot

The cells were plated at a density of $6 \times 10^6$ cells per 100-mm Petri dish in complete medium overnight. Then, the cells were treated with 0–60 μM gefitinib for 24 h. At the end of the treatment, the cells were lysed ice cold cell extract buffer (pH 7.6) containing 0.5 mM DTT, 0.2 mM EDTA, 20 mM HEPES, 2.5 mM $MgCl_2$, 75 mM NaCl, 0.1 mM $Na_3VO_4$, 50 mM NaF, and 0.1% Triton X-100. The following protease inhibitors were added to the cell suspension: 1 μg/ml aprotinin, 0.5 μg/ml leupeptin, and 100 μg/ml 4-(2-aminoethyl) benzenesulfonyl fluoride. The protein concentrations were determined with a BCA protein assay

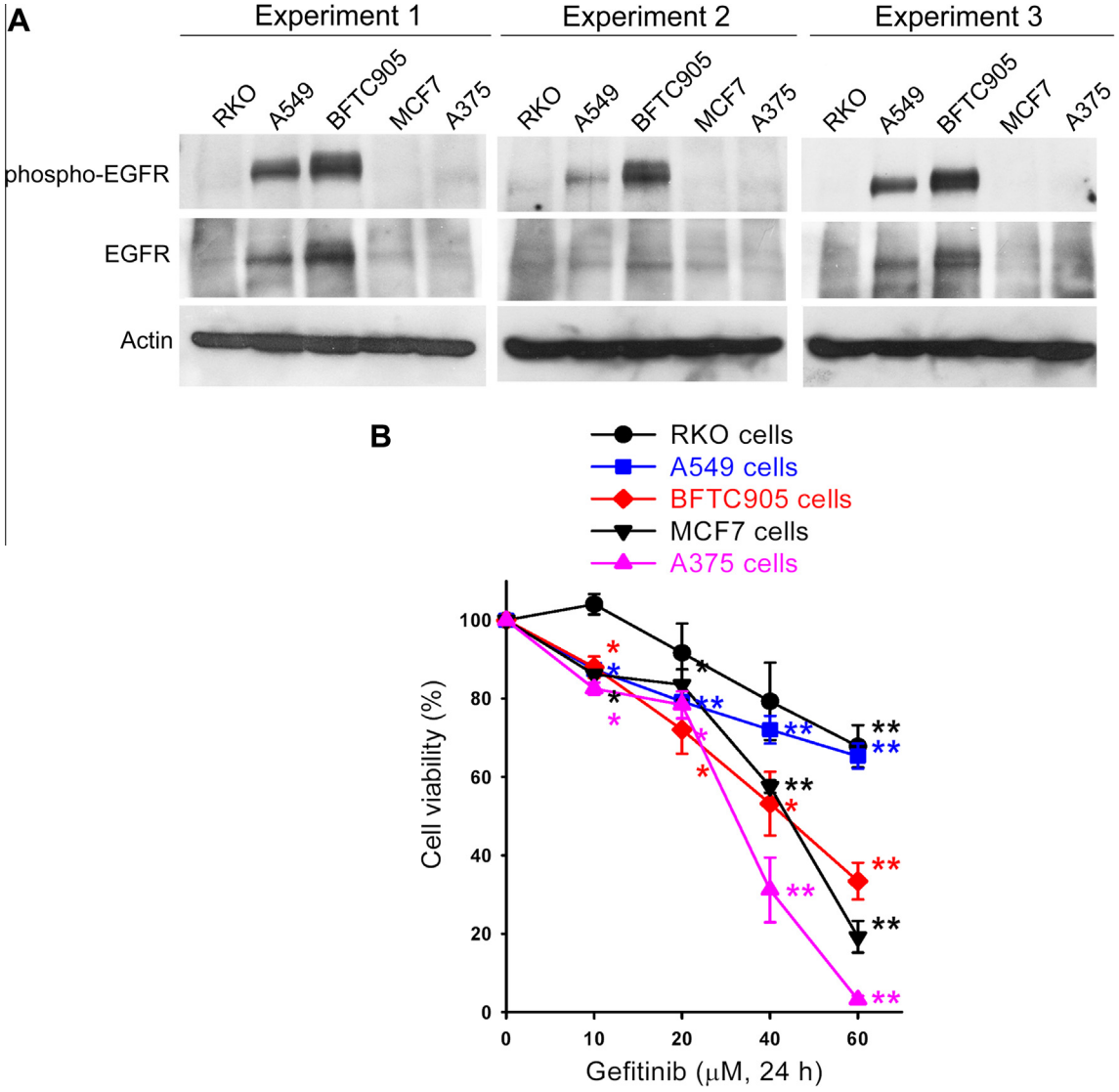


**Fig. 1.** The effect of gefitinib on cell viability in various human cancer cells. (A) The protein levels of phosphorylated and total EGFR in various human cancer cells are shown. The total protein extracts from cancer cell lines including RKO, A549, BFTC905, MCF7 and A375 were subjected to Western blot analysis using specific anti-phospho-EGFR, anti-EGFR and anti-actin antibodies. The Western blot data are shown from three separate experiments with similar findings. Actin was the loading control. (B) The cell lines were treated with 0–60 μM gefitinib for 24 h. After drug treatment, the cells were washed with PBS and incubated for 2 days. The cell viability was measured by MTT assay. The results were obtained from four to seven experiments, and the bar represents the mean ± SE. $^{*}p < 0.05$ and $^{**}p < 0.01$ indicate significant differences between the control and gefitinib treated samples.

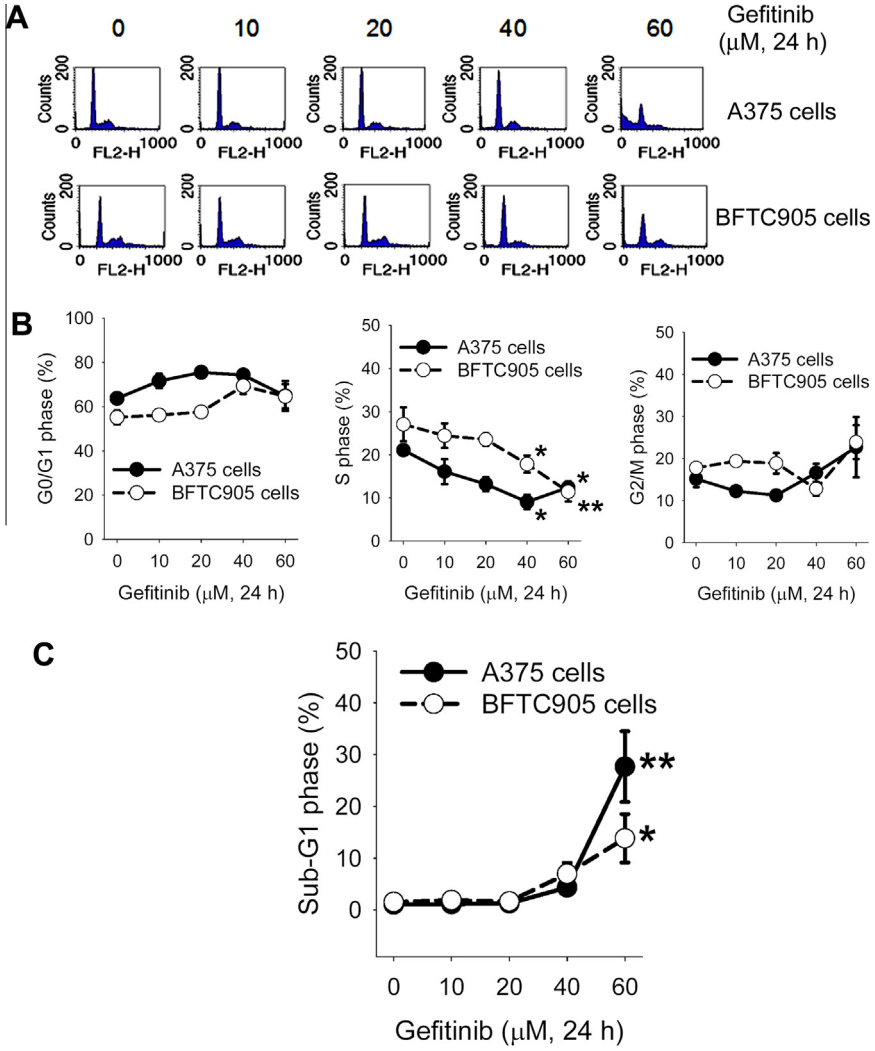


**Fig. 2.** The effect of gefitinib on the cell cycle phase distribution and the sub-G1 population in A375 and BFTC905 cancer cells. (A) The cells were treated with 0–60 μM gefitinib for 24 h. At the end of treatment, the cells were trypsinized and then subjected to flow cytometry analysis. The representative flow data are shown from one of three or four separate experiments with similar findings. (B) The percentages of G0/G1, S, G2/M and sub-G1 fractions were quantified by ModFit LT software. (C) The percentage of cell phase fractions was quantified by CellQuest software. The results were obtained from three to four experiments, and the bar represents the mean ± SE. $^{*}p < 0.05$ and $^{**}p < 0.01$ indicate significant differences between the control and gefitinib treated samples.

kit (Pierce, Rockford, IL). The total cellular protein extracts were prepared. Proteins were separated on 6–12% sodium dodecyl sulfate–polyacrylamide gels, and electrophoretic transfer of proteins onto polyvinylidene difluoride membranes was then performed. The membranes were sequentially hybridized, first with primary antibody and then with a horseradish peroxidase-conjugated secondary antibody. The protein bands were visualized on X-ray film using an enhanced chemiluminescence detection system (PerkinElmer Life and Analytical Sciences, Boston, MA). Western analyses of phospho-EGFR, total EGFR, caspsae-3, PARP, securin, cytochrome c, COX IV and actin were performed using specific antibodies. To verify equal protein loading and transfer, actin and ERK-2 were used as the protein loading controls. Gel digitizing software, Un-Scan-It gel (Ver. 5.1, Silk Scientific, Inc.), was used to semi-quantitatively analyze the intensity of bands on X-ray film.

### 2.10. Immunofluorescence staining and confocal microscopy

To view the localization and expression of securin after gefitinib treatment, the cells were subjected to immunofluorescence staining and confocal microscopy. The night before treatment, the cells were plated on coverslips in 6-well plates at a density of $2 \times 10^5$ per well. After treatment with or without 40 μM gefitinib for 24 h, the cells were washed with isotonic PBS (pH 7.4). Then, the cells were fixed with 4% paraformaldehyde solution for 1 h at 37 °C, followed by three washes with PBS. Non-specific binding sites were blocked using PBS containing 10% FBS and 0.25% Triton X-100 for 1 h at 37 °C, and the blocking solution was removed by washing three times with 0.25% Triton X-100 in PBS. Thereafter, the cells were incubated with mouse anti-securin antibody (1:120) in PBS containing 10% FBS and 0.25% Triton X-100 overnight at 4 °C and were then washed three times with 0.25% Triton X-100 in PBS. Then, the cells were incubated with goat anti-mouse FITC-labeled IgG (1:120) in PBS containing 10% FBS and 0.25% Triton X-100 for 2.5 h at 37 °C and washed three times with 0.25% Triton X-100 in PBS. The β-tubulin and nuclei were stained with the Cy3-labeled anti-β-tubulin and Hoechst 33258, respectively. Finally, the samples were stored in the dark and examined under a confocal microscope system (TCS-SP5-X AOBS, Leica, Germany). The images were acquired with identical exposure conditions using a 63X HCX PL APO 1.4 NA lens and the LAS AF software.

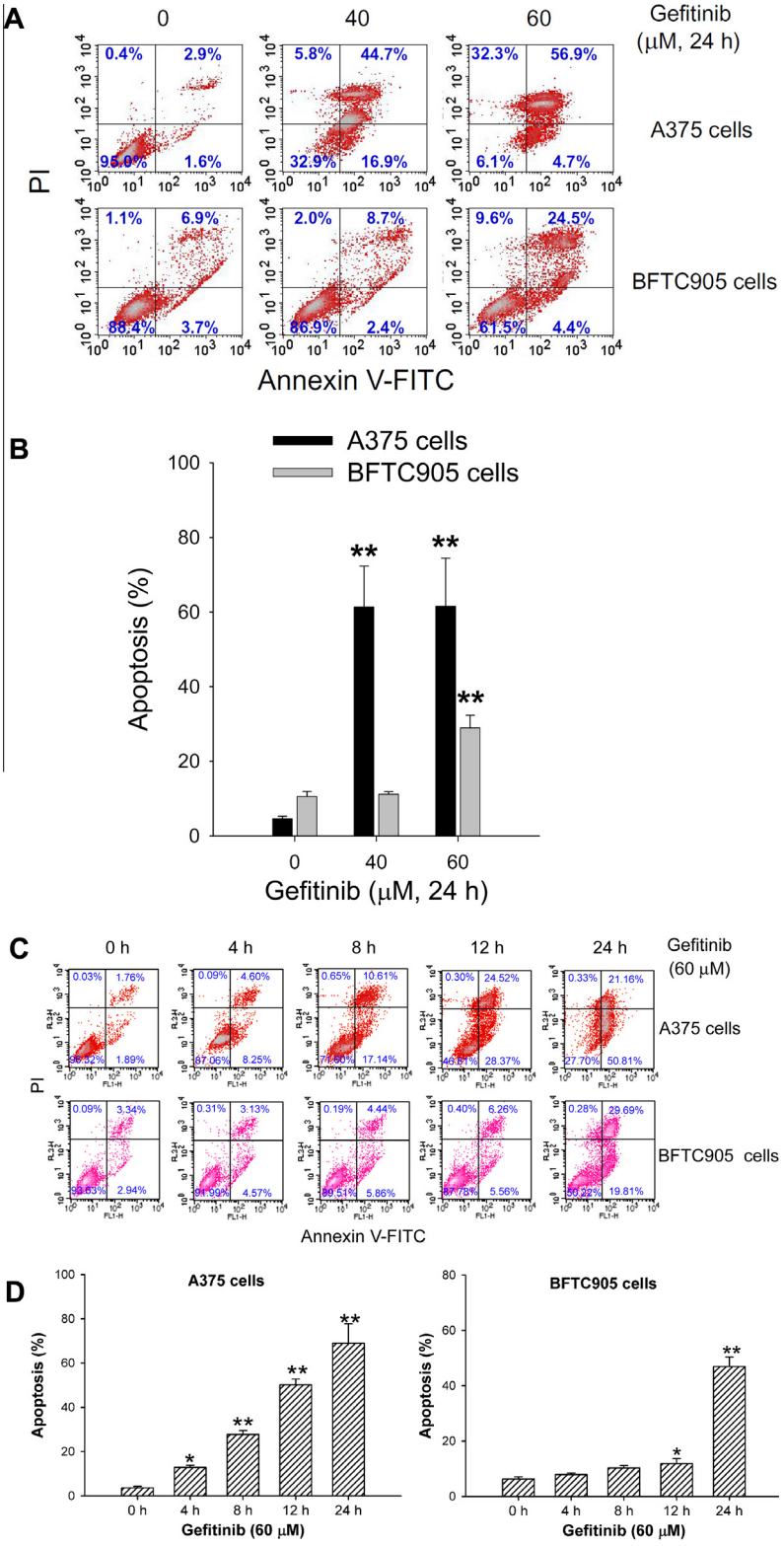


**Fig. 3.** The effect of gefitinib on apoptotic induction in A375 and BFTC905 cancer cells. (A) After treatment with or without gefitinib (40–60 μM) for 24 h, the cells were collected and then subjected to annexin V-FITC and PI staining. The percentage of cellular populations in each quadrant was quantified by CellQuest software. The percentage cells in each quadrant were from the average of three to four independent experiments. (B) The percentage of apoptotic populations (early and late stages) was quantified. The results were obtained from three to four experiments, and the bar represents the mean ± SE. $^{**}p < 0.01$ indicates a significant difference between the control and gefitinib treated samples. (C) A375 and BFTC905 cells were treated with 60 μM gefitinib for time-course observation by annexin V-FITC and PI staining at the indicated times. The percentage cells in each quadrant were from the average of three independent experiments. (D) The percentages of apoptotic populations were quantified. The results were obtained from three experiments, and the bar represents the mean ± SE. $^{*}p < 0.05$ and $^{**}p < 0.01$ indicate a significant difference between the control and gefitinib treated samples.

### 2.11. Reverse transcription-polymerase chain reaction (RT-PCR)

Cells were plated at a density of $2 \times 10^6$ cells per 60-mm Petri dish in culture medium. Total cellular RNA was purified using the Trizol reagent (Invitrogen) according to the manufacturer's protocol. RNA concentrations were determined by spectrophotometry. cDNAs were then synthesized by SuperScriptTM III reverse transcriptase with oligo (dT)12–18 primer (Invitrogen). Each reverse transcript was amplified with GAPDH primers as an internal control. The following primer pairs were used for amplification, securin forward primer: 5′-CCCATATGGCTACTCTGATCT-3′ and securin reverse primer: 5′-GAATATCTATGTCACAGCAAAC-3′ and GAPDH forward primer: 5′-CGGAGTCAACGGATTTGGTCGTAT-3′ and GAPDH reverse primer: 5′-AGCCTTCTCCATGGTGGTGAAGAC-3′. RT-PCR was performed with a DNA thermal cycler (Mastercycler gradient, Hamburg, Germany). The initial denaturation step was

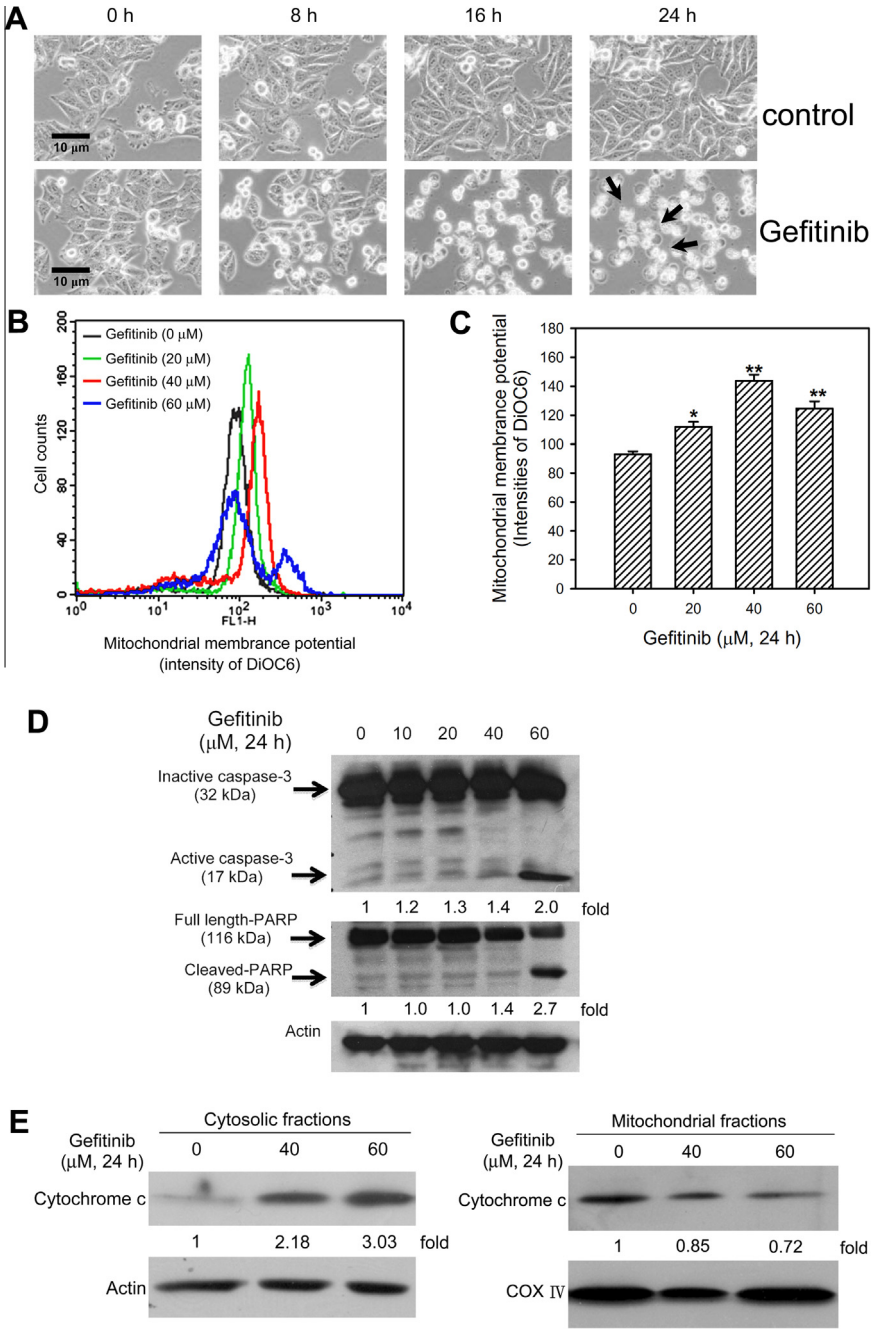


**Fig. 4.** The effect of gefitinib on the induction of mitochondrial hyperpolarization, caspase-3 activation and PARP protein cleavage. (A) A375 cells were plated at a density of $2 \times 10^5$ cells/35-mm Petri dish for 24 h, and then the cells were treated with or without 60 μM gefitinib for 24 h. The cell morphology was observed under a living cell imaging system. The representative cell morphology data are shown from one of three separate experiments with similar findings. The arrows indicate the formation of apoptotic bodies. (B) A375 cells were treated with or without 20–60 μM gefitinib for 24 h, and then the cells were incubated with 50 nM DiOC6 and analyzed by a flow cytometer. (C) The fluorescence intensity of DiOC6 was quantified by CellQuest software. The results were obtained from three to five experiments. The bar represents the mean ± SE. $^*p < 0.05$ and $^{**}p < 0.01$ indicate a significant difference between the control and gefitinib treated samples. (D) The cells were treated with or without 20–60 μM gefitinib for 24 h. The levels of active caspase-3 (17 kDa) and cleaved-PARP (89 kDa) proteins were analyzed by Western blot. Actin was the loading control. The relative protein levels under each treatment were the average of three independent experiments. (E) A375 cells were treated with or without gefitinib. The mitochondrial and cytosolic fractions performed using Mitochondria/Cytosol Fractionation Kit. The total protein extracts were subjected to Western blot analysis using specific antibodies for cytochrome c, COX IV, and actin. The relative protein levels under each treatment were the average of three independent experiments.

performed at 95 °C for 5 min, followed by 25 cycles at 95 °C for 1 min, 56 °C for 1 min, and 72 °C for 1 min, and a final elongation step at 72 °C for 6 min. The PCR products were visualized on ethidium bromide-stained 1.2% agarose gels under UV transillumination, and a photograph was taken with a camera (DH27-S3, Medclub, Taoyuan, Taiwan).

### *2.12. Construction of a green fluorescence protein (GFP)–securin fusion vector*

The full length human securin cDNA was amplified by polymerase chain reaction by a pair of primers (forward: 5′-CATATGGCTACTCTGATCTATGTT-3′ and reverse: 5′-GAATATCTAT-

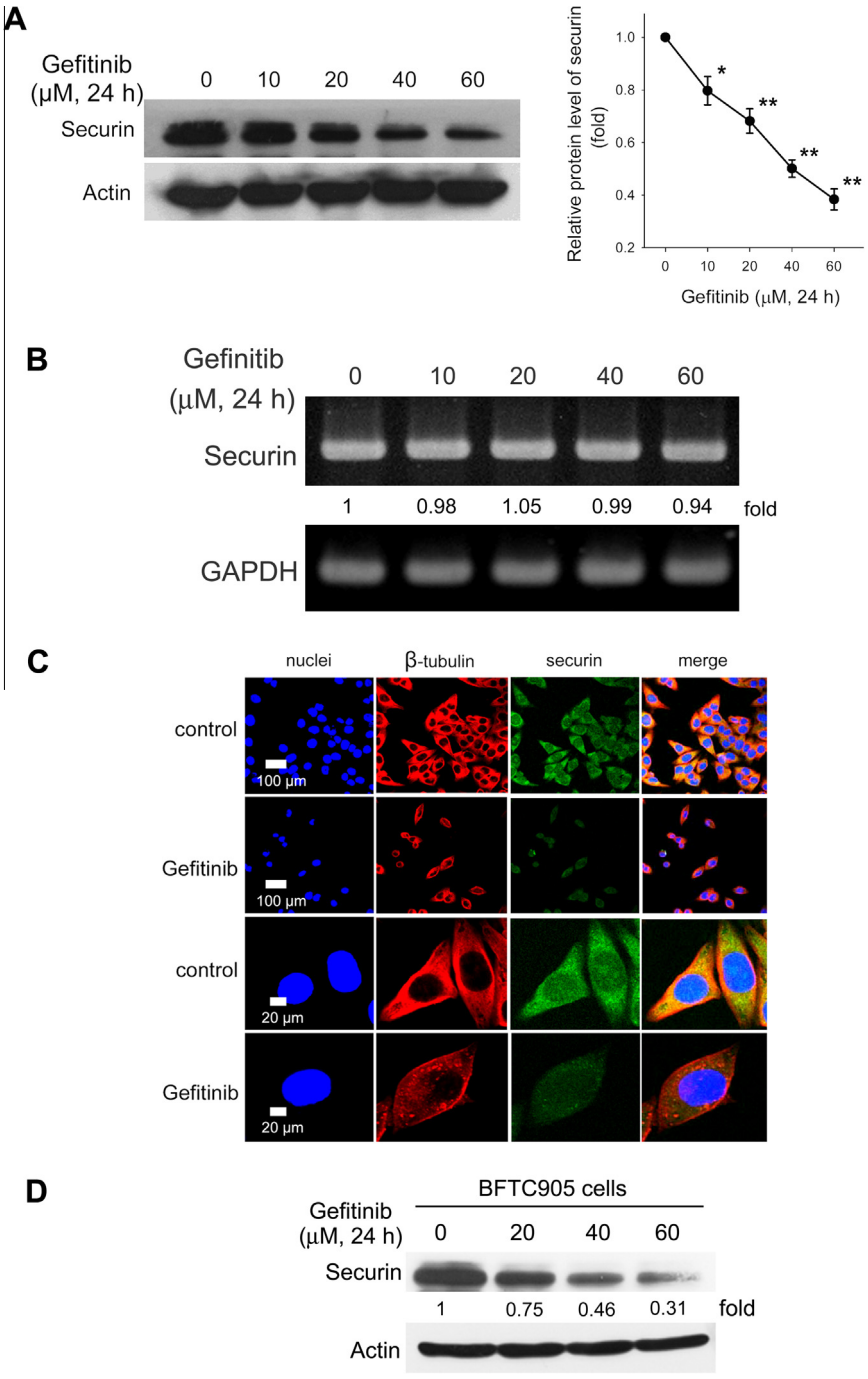


**Fig. 5.** The effect of gefitinib on the securin expression in various cancer cells. (A) A375 cells were treated with 0–60 μM gefitinib for 24 h. The total protein extracts were prepared for immunoblot analysis using anti-securin and anti-actin antibodies. Actin was used as a loading control. The results were obtained from three independent experiments, and the bar represents the mean ± SE. $^{*}p < 0.05$ and $^{**}p < 0.01$ indicate a significant difference between the control and gefitinib treated samples. (B) The cells were treated with 0–60 μM gefitinib for 24 h. The cells were harvested and analyzed by RT-PCR to determine the securin mRNA levels. The relative mRNA levels under each treatment were the average of three independent experiments. (C) The cells were treated with or without 40 μM gefitinib for 24 h. At the end of treatment, the cells were incubated with mouse anti-securin antibody and then incubated with goat anti-mouse FITC. The β-tubulin and nuclei were stained with the Cy3-labeled anti-β-tubulin antibody and Hoechst 33258 dye, respectively. Images were acquired with identical exposure conditions and analyzed by a confocal microscope system. (D) BFTC905 cells were treated with 0–60 μM gefitinib for 24 h. The total protein extracts were prepared for immunoblot analysis using anti-securin and anti-actin antibodies. The relative protein levels under each treatment were the average of three independent experiments.

GTCACAGCAAAC-3′). The securin cDNA fragment was cloned into a CT–GFP TOPO vector using a CT–GFP fusion TOPO expression kit (K4820-101, Invitrogen) according to the manufacturer's recommendations. The successful clones of the securin-expression vectors in *Escherichia coli* (BL21 DE3) were confirmed by DNA sequencing. One of the successful GFP–securin expression vectors was named pCT–GFP–securin, and the control vector was named pCT–GFP.

### 2.13. Transfection

Control vector (pCT–GFP) and pCT–GFP–securin were employed for transfection using Lipofectamine™ 2000 (Invitrogen) according to the manufacturer's recommendations. The cells were plated in 96-well plates at a density of $8 \times 10^3$ cells per well in complete medium overnight. The cells were then transfected with 50 μg/ml of control or securin-expression vector in serum-free medium for 6 h at 37 °C. An equal amount of medium containing 20% FBS was added without removing the transfection mixture, and incubation proceeded for an additional 24 h. After the vector transfections, the cells were subjected to MTT and Western blot assays, as described above.

### 2.14. Statistical analysis

Each experiment was repeated at least three times. The data from the populations of cells under different treatment conditions were analyzed using paired Student's *t*-test. In a comparison of multiple groups, the data were analyzed by one-way or two-way analysis of variance (ANOVA) and further analyzed by post Tukey's tests using the statistics software GraphPad Prism 5 (GraphPad software, Inc. San Diego, CA). A $p$ value of <0.05 was considered to be statistically significant in each experiment.

## 3. Results

### 3.1. Gefitinib reduces cell viability in the EGFR-deficient and EGFR-expressing human cancer cell lines

The protein expression of phospho-EGFR and total EGFR in a variety of human cancer cell lines including RKO, A549, BFTC905, MCF7 and A375 were analyzed by Western blot. BFTC905 and A549 cells expressed relatively high levels of the phosphorylated EGFR and total EGFR proteins; in contrast, A375, MCF7, and RKO cells did not markedly express those proteins (Fig. 1A). Actin served as an internal loading control protein. We have examined the cell viability following treatment with gefitinib (10–60 μM for 24 h) in the above cell lines. Gefitinib significantly reduced cell viability in a concentration-dependent manner in both the EGFR-deficient and EGFR-expressing cancer cell lines (Fig. 1B). The EGFR-deficient A375 cells displayed the most sensitivity among the five cancer cell lines regarding cell viability in response to gefitinib treatment at concentrations from 40–60 μM (Fig. 1B).

### 3.2. Gefitinib induces apoptosis in A375 and BFTC905 cancer cell lines

To investigate the induction of apoptosis by gefitinib in the EGFR-deficient and EGFR-expressing cancer cell lines, A375 and BFTC905 cells were compared and analyzed by the abundance of sub-G1 fractions and annexin V-FITC and PI staining. Treatment with 60 μM gefitinib for 24 h increased the sub-G1 fractions to 26.6% and 12.3% in A375 and BFTC905 cancer cells, respectively (Fig. 2A and 2C). The levels of apoptosis following gefitinib treatment (40–60 μM for 24 h or 60 μM for 4–24 h) were further examined by annexin V-FITC and PI staining. The numbers of annexin V (+)/PI (−) cells (early apoptosis) and annexin V (+)/PI (+) cells (late apoptosis) were significantly increased by treatment with 60 μM gefitinib in both the A375 and BFTC905 cancer cells (Fig. 3A and B). Treatment with 60 μM gefitinib for 24 h induced total apoptosis of approximately 61.6% and 28.9% of the population in A375 and BFTC905 cells, respectively. In addition, the total apoptotic levels were significantly increased following gefitinib treatment in a time-dependent manner in both the A375 and BFTC905 cancer cells (Fig. 3C and D). Furthermore, gefitinib (40–60 μM) reduced the fraction of cells in S phase in A375 and BFTC905 cancer cells (Fig. 2B, $p < 0.05$). However, gefitinib did not alter the levels of G0/G1 and G2/M fractions in these cells (Fig. 2B, $p > 0.05$).

### 3.3. Gefitinib induces the hyperpolarization of mitochondria and elevates the activation of caspase-3 and the protein cleavage of PARP

The time-lapse observation of cell death morphology by treatment with 60 μM gefitinib for 8–24 h in A375 cells was recorded (Fig. 4A). Gefitinib induced the morphological alterations, including the round-up morphology, the cell membrane blebbing and the formation of apoptotic bodies under phase contrast microscope (Fig. 4A). Furthermore, treatment with 20–60 μM gefitinib for 24 h significantly increased the intensity of DiOC6 (Fig. 4B and C). Gefitinib (60 μM, 24 h) markedly increased the protein levels of active caspase-3 (17 kDa) and cleaved PARP (89 kDa) ($p < 0.01$), which further demonstrates an increase in apoptosis in these cells (Fig. 4D). Moreover, gefitinib increased the amount of cytochrome c in the cytosolic fractions but conversely reduced in the mitochondrial fractions (Fig. 4E). Actin was used as a loading control in cytosolic fractions. COX IV was used as a loading control for mitochondrial fractions. The protein levels of actin and COX IV were not altered by gefitinib (Fig. 4E).

### 3.4. Gefitinib treatment inhibits securin protein expression in cancer cells

To study the role of securin in gefitinib-induced apoptosis in cancer cells, the expression of securin after treatment with gefitinib was analyzed by Western blot and RT-PCR. Treatment with 10–60 μM gefitinib for 24 h significantly inhibited securin protein levels in A375 cells (Fig. 5A). In addition to A375 cells, gefitinib could reduce securin protein levels in BFTC905 cells (Fig. 5D) and other cancer cell lines (RKO and A549) (data not shown). However,

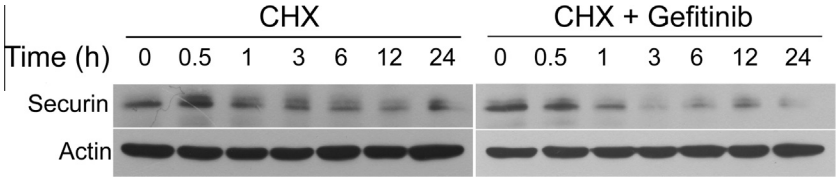


**Fig. 6.** Gefitinib induces the securin protein instability of human cancer cells. A375 cells were co-treated with or without 60 μM gefitinib and 10 μg/ml cycloheximide (CHX) for 0–24 h. The treated cells were harvested at the indicated times for Western blot assays. The representative Western blot data were shown from one of three separate experiments with similar findings.

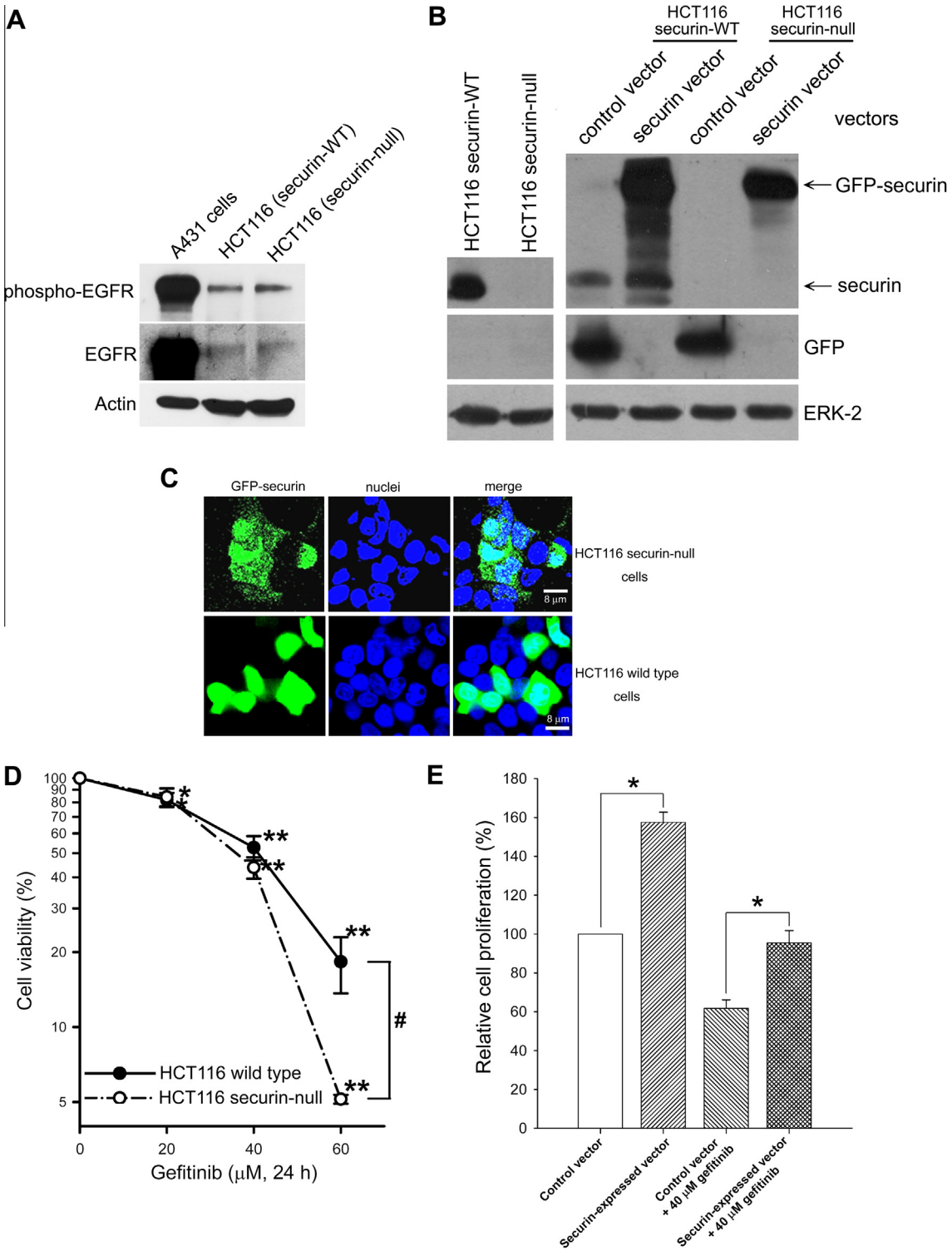


**Fig. 7.** Overexpression of securin by a GFP–securin expression vector shows increased resistance to the gefitinib-induced cancer cell death. (A) The total protein extracts from HCT116 securin-wild type and securin-null cells were subjected to Western blot assays using anti-phospho-EGFR, anti-EGFR and anti-actin antibodies. Protein extracts from A431 cells served as a positive control for phospho-EGFR and EGFR levels. (B) HCT116 securin-wild type or securin-null cells were transfected with 10 μg control vector (pCT–GFP) or GFP–securin expression vector (pCT–GFP–securin). The total protein extracts were subjected to Western blot analysis. (C) HCT116 securin-wild type or securin-null cells were transfected with 10 μg pCT–GFP–securin vector. After transfection, the fluorescence of GFP–securin proteins was observed under a confocal microscope. The nuclei were stained with Hoechst 33258, which displayed a blue color. The securin–GFP proteins emitted the green fluorescence. (D) HCT116 securin-wild type or securin-null cells were treated with 0–60 μM gefitinib for 24 h. After drug treatment, the cells were washed with PBS and incubated for 2 days. The cell viability was measured by an MTT assay. The results were obtained from six experiments. The bar represents the mean ± SE. $^{*}p < 0.05$ and $^{**}p < 0.01$ indicate a significant difference between the control and gefitinib treated samples. $^{\#}p < 0.05$ indicates a significant difference between the securin-wild type and securin-null HCT116 cancer cells, which were treated with the same gefitinib concentration. (E) A375 cells were transfected with the control or securin–GFP expression vector and then treated with or without 40 μM gefitinib for 24 h. At the end of treatment, the cells were washed with PBS and incubated for 2 days. The relative cellular proliferation following the treatments was compared using MTT assays. The results were obtained from four experiments, and the bar represents the mean ± SE. $^{*}p < 0.05$ indicates a significant difference between the control and securin–GFP expressing samples.

treatment with gefitinib did not markedly decrease the securin mRNA levels in those cancer cells (Fig. 5B). GAPDH served as an internal control gene. Moreover, the intensities of green fluorescence (FITC), observed by immunofluorescence staining and confocal microscopy analysis, showed that securin protein levels were decreased in A375 cells following treatment with gefitinib (Fig. 5C).

To further examine the protein stability of securin following gefitinib treatment, the cells were co-treated with a protein synthesis inhibitor, cycloheximide. The securin protein degradation rate was faster after co-treatment with gefitinib and cycloheximide than it was with cycloheximide treatment alone over a 6–24 h period (Fig. 6).

### 3.5. Overexpression of securin promotes cancer cell proliferation and resistance to gefitinib-induced apoptosis

To determine the expression of phospho-EGFR and total EGFR in securin-wild type and securin-null cancer cells, we compared securin-wild type and securin-null HCT116 colorectal cancer cells. Interestingly, the securin-wild type and the securin-null HCT116 colorectal cancer cells expressed comparable levels of both the phosphorylated EGFR and total EGFR proteins (Fig. 7A). The A431 cell line was used as an EGFR positive control that expressed high levels of both phosphorylated and total EGFR proteins (Fig. 7A). We further constructed a securin expression vector (pCT–GFP–securin) to study the role of securin in controlling gefitinib-induced apoptosis. Immunoblot analysis, using a specific anti-securin antibody in the securin-wild type and securin-null cells showed that transfection with the pCT–GFP–securin vector expressed a GFP–securin fusion protein (49 kDa) (Fig. 7B). The endogenous securin proteins in HCT116 wild type cells were recognized as 22 kDa proteins (Fig. 7B). The control pCT–GFP vector expressed the GFP protein (27 kDa). ERK-2 was used as an internal control protein that was not altered by the transfections. Fig. 7C shows the cellular protein location of GFP–securin (green color) in the securin-wild type or securin-null cells after transfection with the pCT–GFP–securin vector. The cell viability was reduced to 18.3% and 5.1% in securin-wild type and securin-null cells, respectively, following treatment with 60 μM gefitinib for 24 h (Fig. 7D). The securin-null cells exhibited greater cytotoxicity (∼13%) than the securin-wild type cells in response to gefitinib treatment. Furthermore, overexpression of securin by the pCT–GFP–securin vector increased proliferation by ∼60% in A375 cells (Fig. 7E). In addition, transfection of the pCT–GFP–securin vector conferred resistance to gefitinib-induced cell death compared to the control vector (Fig. 7E).

## 4. Discussion

Gefitinib has been used to treat various human cancers [6,7]. However, several reports indicate that cancer cells can become resistant to gefitinib and other EGFR inhibitors during cancer therapy [11–14]. Elucidating the mechanisms of resistance to such drugs in cancer cells will be beneficial for cancer patient treatment using EGFR inhibitors. It has been shown that the T790M mutation in EGFR causes drug resistance by increasing the binding affinity for ATP [15]. In the present study, we provide evidence that securin can confer resistance to gefitinib-induced apoptosis in human cancer cells. Securin has been shown to be highly expressed in numerous human cancers [21,23–26], and its levels correlate with tumorigenesis, cancer metastasis [21,22,30–32], and poor prognosis in response to cancer therapy [33,34]. Furthermore, the depletion of securin can enhance cancer cell death toward chemosensitivity [27,28,37] or radiosensitivity [29]. Our results indicate that the loss of securin protein in cancer cells may increase sensitivity to the induction of cytotoxicity and apoptosis by gefitinib treatment. Conversely, the vector-based expression of securin provides evidence that demonstrate that securin can reduce the gefitinib-induced apoptosis. These findings imply that the presence of securin in cancers may promote resistance to gefitinib during cancer therapy.

It has been reported that EGFR is related to securin gene expression and enhanced proliferating cell nuclear antigen in pituitary folliculostellate cells [35]. Gefitinib can inhibit EGF-induced securin expression and cellular proliferation [35]. Additionally, AG1478, another specific EGFR inhibitor, can also block the induction of securin [36]. We found that gefitinib reduced securin protein expression but did not alter the gene expression of securin. Gefitinib reduced securin protein expression, indicating an increase of protein instability. Furthermore, gefitinib induced apoptosis and reduced the securin protein expression in both EGFR-deficient and EGFR-expressing cells. In addition, the securin-wild type and securin-null cancer cells expressed both phosphorylated EGFR and total EGFR proteins to a similar degree. Thus, we suggest that gefitinib induces apoptosis related to the reduction of securin through an EGFR-independent pathway in human cancer cells.

Blockage of securin has been shown to trigger cancer cell death [27,28,37]. It has been reported that gefitinib induces apoptosis in various cancer cells [8–10]. Caspases are central effectors of apoptosis [38]. PARP is one of the prime target proteins for caspase-3 [39]. Apoptosis is associated with early mitochondrial hyperpolarization, cytochrome c release and caspase-3 activation [40–42]. We found that gefitinib induced mitochondrial hyperpolarization and cytochrome c release from mitochondria to cytosol in human cancer cells. Gefitinib further increased caspase-3 activation and PARP protein cleavage. Subsequently, gefitinib induced apoptosis in both EGFR-deficient and EGFR-expressed cancer cell lines. Accordingly, we suggest that gefitinib can induce apoptosis through mitochondrial dysfunction, caspase-3 activation and PARP cleavage in an EGFR-independent pathway.

p53, a well-known tumor suppressor, regulates cell cycle arrest and apoptosis [43–45]. It is well characterized that numerous cancers are caused by the mutations of p53. The loss of functional p53 in cancer cells may resist to chemotherapy and radiotherapy of cancers. It has been reported that acquired resistance to EGFR inhibitors is associated with the loss of p53 in human cancers [11]. Securin can interact with p53, which prevents p53-mediated apoptosis in cancer cells by blocking the transcriptional activity of p53 [46]. In contrast, the activation of p53 can inhibit securin expression following treatment with anticancer drugs such as oxaliplatin [47]. It is possible that securin and p53 play a crucial role in the regulation of gefitinib resistance in human cancer cells. Accordingly, the loss of p53 or the increase of securin in cancer cells may elevate the resistance of gefitinib in cancer patients.

In summary, we elucidated the novel role of securin in promoting resistance to gefitinib therapy in cancer cells. Securin confers resistance to gefitinib-induced apoptosis in an EGFR-independent pathway. Understanding the mechanisms by which securin modulates gefitinib-induced cancer cell death may contribute to the development of novel therapeutic strategies targeting such disease states.

## Conflict of interest statement

None declared.

## Acknowledgements

We thank Dr. B. Vogelstein of The Johns Hopkins University for providing securin-wild type and securin-null HCT116 colorectal

cancer cells. The authors also gratefully thank the Multiphoton and Confocal Microscope System core facility of National Chiao University. This work was supported by grants from NSC 96-2311-B-320-006-MY3, NSC 100-2627-B-009-007 and NSC 101-2627-B-009-006 of National Science Council, Taiwan.

## References

[1] A. Citri, Y. Yarden, EGF–ERBB signalling: towards the systems level, Nat. Rev. Mol. Cell Biol. 7 (2006) 505–516.
[2] M. Sibilia, R. Kroismayr, B.M. Lichtenberger, A. Natarajan, M. Hecking, M. Holcmann, The epidermal growth factor receptor: from development to tumorigenesis, Differentiation 75 (2007) 770–787.
[3] J.R. Grandis, J.C. Sok, Signaling through the epidermal growth factor receptor during the development of malignancy, Pharmacol. Ther. 102 (2004) 37–46.
[4] J.G. Paez, P.A. Janne, J.C. Lee, S. Tracy, H. Greulich, S. Gabriel, P. Herman, F.J. Kaye, N. Lindeman, T.J. Boggon, K. Naoki, H. Sasaki, Y. Fujii, M.J. Eck, W.R. Sellers, B.E. Johnson, M. Meyerson, EGFR mutations in lung cancer: correlation with clinical response to gefitinib therapy, Science 304 (2004) 1497–1500.
[5] P.R. Dutta, A. Maity, Cellular responses to EGFR inhibitors and their relevance to cancer therapy, Cancer Lett. 254 (2007) 165–177.
[6] G. Lurje, H.J. Lenz, EGFR signaling and drug discovery, Oncology 77 (2009) 400–410.
[7] F. Ciardiello, G. Tortora, EGFR antagonists in cancer treatment, N. Engl. J. Med. 358 (2008) 1160–1174.
[8] M. Ono, A. Hirata, T. Kometani, M. Miyagawa, S. Ueda, H. Kinoshita, T. Fujii, M. Kuwano, Sensitivity to gefitinib (Iressa, ZD1839) in non-small cell lung cancer cell lines correlates with dependence on the epidermal growth factor (EGF) receptor/extracellular signal-regulated kinase 1/2 and EGF receptor/Akt pathway for proliferation, Mol. Cancer Ther. 3 (2004) 465–472.
[9] F. Ciardiello, R. Caputo, R. Bianco, V. Damiano, G. Pomatico, S. De Placido, A.R. Bianco, G. Tortora, Antitumor effect and potentiation of cytotoxic drugs activity in human cancer cells by ZD-1839 (Iressa), an epidermal growth factor receptor-selective tyrosine kinase inhibitor, Clin. Cancer Res. 6 (2000) 2053–2063.
[10] F.M. Sirotnak, M.F. Zakowski, V.A. Miller, H.I. Scher, M.G. Kris, Efficacy of cytotoxic agents against human tumor xenografts is markedly enhanced by coadministration of ZD1839 (Iressa), an inhibitor of EGFR tyrosine kinase, Clin. Cancer Res. 6 (2000) 4885–4892.
[11] S. Huang, S. Benavente, E.A. Armstrong, C. Li, D.L. Wheeler, P.M. Harari, P53 modulates acquired resistance to EGFR inhibitors and radiation, Cancer Res. 71 (2011) 7071–7079.
[12] D. Jackman, W. Pao, G.J. Riely, J.A. Engelman, M.G. Kris, P.A. Janne, T. Lynch, B.E. Johnson, V.A. Miller, Clinical definition of acquired resistance to epidermal growth factor receptor tyrosine kinase inhibitors in non-small-cell lung cancer, J. Clin. Oncol. 28 (2010) 357–360.
[13] D.L. Wheeler, E.F. Dunn, P.M. Harari, Understanding resistance to EGFR inhibitors-impact on future treatment strategies, Nat. Rev. Clin. Oncol. 7 (2010) 493–507.
[14] J.A. Engelman, P.A. Janne, Mechanisms of acquired resistance to epidermal growth factor receptor tyrosine kinase inhibitors in non-small cell lung cancer, Clin. Cancer Res. 14 (2008) 2895–2899.
[15] C.H. Yun, K.E. Mengwasser, A.V. Toms, M.S. Woo, H. Greulich, K.K. Wong, M. Meyerson, M.J. Eck, The T790M mutation in EGFR kinase causes drug resistance by increasing the affinity for ATP, Proc. Natl. Acad. Sci. USA 105 (2008) 2070–2075.
[16] H. Zou, T.J. McGarry, T. Bernal, M.W. Kirschner, Identification of a vertebrate sister-chromatid separation inhibitor involved in transformation and tumorigenesis, Science 285 (1999) 418–422.
[17] A. Dominguez, F. Ramos-Morales, F. Romero, R.M. Rios, F. Dreyfus, M. Tortolero, J.A. Pintor-Toro, Hpttg, a human homologue of rat pttg, is overexpressed in hematopoietic neoplasms, Evidence for a transcriptional activation function of hPTTG, Oncogene 17 (1998) 2187–2193.
[18] G. Vlotides, T. Eigler, S. Melmed, Pituitary tumor-transforming gene: physiology and implications for tumorigenesis, Endocr. Rev. 28 (2007) 165–186.
[19] J. Mei, X. Huang, P. Zhang, Securin is not required for cellular viability, but is required for normal growth of mouse embryonic fibroblasts, Curr. Biol. 11 (2001) 1197–1201.
[20] P.V. Jallepalli, I.C. Waizenegger, F. Bunz, S. Langer, M.R. Speicher, J.M. Peters, K.W. Kinzler, B. Vogelstein, C. Lengauer, Securin is required for chromosomal stability in human cells, Cell 105 (2001) 445–457.
[21] F. Salehi, K. Kovacs, B.W. Scheithauer, R.V. Lloyd, M. Cusimano, Pituitary tumor-transforming gene in endocrine and other neoplasms: a review and update, Endocr. Relat. Cancer 15 (2008) 721–743.
[22] X. Zhang, G.A. Horwitz, T.R. Prezant, A. Valentini, M. Nakashima, M.D. Bronstein, S. Melmed, Structure, expression, and function of human pituitary tumor-transforming gene (PTTG), Mol. Endocrinol. 13 (1999) 156–166.
[23] A.P. Heaney, R. Singson, C.J. McCabe, V. Nelson, M. Nakashima, S. Melmed, Expression of pituitary-tumour transforming gene in colorectal tumours, Lancet 355 (2000) 716–719.
[24] C. Solbach, M. Roller, C. Fellbaum, M. Nicoletti, M. Kaufmann, PTTG mRNA expression in primary breast cancer: a prognostic marker for lymph node invasion and tumor recurrence, Breast 13 (2004) 80–81.
[25] S.S. Kakar, M.T. Malik, Suppression of lung cancer with siRNA targeting PTTG, Int. J. Oncol. 29 (2006) 387–395.
[26] R. Puri, A. Tousson, L. Chen, S.S. Kakar, Molecular cloning of pituitary tumor transforming gene 1 from ovarian tumors and its expression in tumors, Cancer Lett. 163 (2001) 131–139.
[27] J.I. Chao, S.H. Hsu, T.C. Tsou, Depletion of securin increases arsenite-induced chromosome instability and apoptosis via a p53-independent pathway, Toxicol. Sci. 90 (2006) 73–86.
[28] J.I. Chao, H.F. Liu, The blockage of survivin and securin expression increases the cytochalasin B-induced cell death and growth inhibition in human cancer cells, Mol. Pharmacol. 69 (2006) 154–164.
[29] W.S. Chen, Y.C. Yu, Y.J. Lee, J.H. Chen, H.Y. Hsu, S.J. Chiu, Depletion of securin induces senescence after irradiation and enhances radiosensitivity in human cancer cells regardless of functional p53 expression, Int. J. Radiat. Oncol. Biol. Phys. 77 (2010) 566–574.
[30] T. Hamid, M.T. Malik, S.S. Kakar, Ectopic Expression of PTTG1/securin promotes tumorigenesis in human embryonic kidney cells, Mol. Cancer 4 (2005) 3.
[31] K. Boelaert, C.J. McCabe, L.A. Tannahill, N.J. Gittoes, R.L. Holder, J.C. Watkinson, A.R. Bradwell, M.C. Sheppard, J.A. Franklyn, Pituitary tumor transforming gene and fibroblast growth factor-2 expression: potential prognostic indicators in differentiated thyroid cancer, J. Clin. Endocrinol. Metab. 88 (2003) 2341–2347.
[32] K. Talvinen, H. Karra, S. Hurme, M. Nykanen, A. Nieminen, J. Anttinen, T. Kuopio, P. Kronqvist, Securin promotes the identification of favourable outcome in invasive breast cancer, Br. J. Cancer 101 (2009) 1005–1010.
[33] S.T. Avoranta, E.A. Korkeila, H.R. Minn, K.J. Syrjanen, S.O. Pyrhonen, J.T. Sundstrom, Securin identifies a subgroup of patients with poor outcome in rectal cancer treated with long-course (chemo) radiotherapy, Acta Oncol. 50 (2011) 1158–1166.
[34] H. Karra, R. Pitkanen, M. Nykanen, K. Talvinen, T. Kuopio, M. Soderstrom, P. Kronqvist, Securin predicts aneuploidy and survival in breast cancer, Histopathology 60 (2012) 586–596.
[35] G. Vlotides, M. Cruz-Soto, T. Rubinek, T. Eigler, C.J. Auernhammer, S. Melmed, Mechanisms for growth factor-induced pituitary tumor transforming gene-1 expression in pituitary folliculostellate TtT/GF cells, Mol. Endocrinol. 20 (2006) 3321–3335.
[36] J. Tfelt-Hansen, S. Yano, S. Bandyopadhyay, R. Carroll, E.M. Brown, N. Chattopadhyay, Expression of pituitary tumor transforming gene (PTTG) and its binding protein in human astrocytes and astrocytoma cells: function and regulation of PTTG in U87 astrocytoma cells, Endocrinology 145 (2004) 4222–4231.
[37] S.H. Yu, P.M. Yang, C.W. Peng, Y.C. Yu, S.J. Chiu, Securin depletion sensitizes human colon cancer cells to fisetin-induced apoptosis, Cancer Lett. 300 (2011) 96–104.
[38] Y. Shi, Mechanisms of caspase activation and inhibition during apoptosis, Mol. Cell 9 (2002) 459–470.
[39] D.K. Miller, The role of the caspase family of cysteine proteases in apoptosis, Semin. Immunol. 9 (1997) 35–49.
[40] M. Poppe, C. Reimertz, H. Dussmann, A.J. Krohn, C.M. Luetjens, D. Bockelmann, A.L. Nieminen, D. Kogel, J.H. Prehn, Dissipation of potassium and proton gradients inhibits mitochondrial hyperpolarization and cytochrome c release during neural apoptosis, J. Neurosci. 21 (2001) 4551–4563.
[41] A. Gross, J.M. McDonnell, S.J. Korsmeyer, BCL-2 family members and the mitochondria in apoptosis, Genes Dev. 13 (1999) 1899–1911.
[42] P.W. Hsiao, C.C. Chang, H.F. Liu, C.M. Tsai, T.H. Chiu, J.I. Chao, Activation of p38 mitogen-activated protein kinase by celecoxib oppositely regulates survivin and gamma-H2AX in human colorectal cancer cells, Toxicol. Appl. Pharmacol. 222 (2007) 97–104.
[43] S. Bates, K.H. Vousden, P53 in signaling checkpoint arrest or apoptosis, Curr. Opin. Genet. Dev. 6 (1996) 12–18.
[44] A.J. Levine, P53, the cellular gatekeeper for growth and division, Cell 88 (1997) 323–331.
[45] L.J. Hofseth, S.P. Hussain, C.C. Harris, P53: 25 years after its discovery, Trends Pharmacol. Sci. 25 (2004) 177–181.
[46] J.A. Bernal, R. Luna, A. Espina, I. Lazaro, F. Ramos-Morales, F. Romero, C. Arias, A. Silva, M. Tortolero, J.A. Pintor-Toro, Human securin interacts with p53 and modulates p53-mediated transcriptional activity and apoptosis, Nat. Genet. 32 (2002) 306–311.
[47] S.J. Chiu, T.S. Hsu, J.I. Chao, Opposing securin and p53 protein expression in the oxaliplatin-induced cytotoxicity of human colorectal cancer cells, Toxicol. Lett. 167 (2006) 122–130.